Corrosion behaviour study of heat-resistant steel under oxidation and reduction atmosphere

Corrosion behaviour study of heat-resistant steel under oxidation and reduction atmosphere

Hong Xu[1], Sicong Zhang [2,4], Shangkun Zhou [2], Weigang Xu[3] and Houzhang Tan[2]

[1] Jiangsu Frontier Electric Technology Co.LTD, Nanjing, Jiangsu;
[2] Key Laboratory of Thermal Flow Science and Engineering, Ministry of Education, Xi'an Jiaotong University, Xi'an, Shaanxi;
[3] Changzhou University, Changzhou, Jiangsu.

[4] Email: sczhang@stu.xjtu.edu.cn

Abstract. High-temperature corrosion is one of the main problems that plague the safe operation of thermal power plants. Especially for units burning high-sulfur coal, the probability of high-temperature corrosion is much greater than that of units burning low-sulfur coal. In this paper, the 12Cr1MoV steel used in power plants is selected as the research object, the experiment studied the corrosion behavior of H_2S, SO_2 and air in the temperature range of 400-500℃. We found that 12Cr1MoV has the highest corrosion rate in the H_2S atmosphere, the second in the air, and the slowest in the SO_2 atmosphere.

1. Introduction

With the tightening of environmental emission standards, more and more thermal power plants have implemented ultra-low emission standards and strictly controlled nitrogen dioxide emissions below 50 mg/m^3. The large power station boiler with subcritical parameters have higher temperature of water wall. The application of low NOx staged combustion technology makes the main combustion area in a lean oxygen state, and the reducing atmosphere near the surface of the water wall is more intense, which leads to high-temperature corrosion and thinning of the water wall tube. Once it is operated for a long time, it will cause steam leakage accidents in the pipe, leading abnormal shutdowns of the unit, bringing economic losses to the power generation enterprise, and threatening the safe operation of the power grid.

In terms of mechanism research, Cain [1] pointed out that alkaline metal trisulfate needs to be formed in an environment of at least 250 ppm SO_3. Nalson [2] found that the mixture of trisulfate compounds of alkali metals such as Na, K has a melting temperature lower than that of the pure substance, and can even be as low as 477℃. Hedly et al. [3] pointed out that SO_3 has insufficient retention time due to the reaction in the furnace, so the conversion rate is between 1.5 and 2%, and it hardly exceeds this range. Krause et al. [4] clearly indicated that the evidence for the formation of alkaline trisulfate compounds by SO_3 (1.5~2%) at this concentration is insufficient. Schofield [5] proposed a new method for reducing the high-temperature corrosion of sulfur and chlorine deposits using tungsten salts during combustion. Latham [6] proved through experiments that there is a good coupling relationship between chlorine and alkali metals. Krause [7-9] proved through experiments that the chemical corrosion of Cl_2 began at about 204℃, and the melting point of $FeCl_2$ is very low, which is a volatile substance. However, Cl_2 will cause severe corrosion to the metal only when the metal temperature reaches above 508℃. Lee [10] pointed out that $FeCl_2$ has a specific volume

equivalent to about 11 times the reaction metal, so it is easy to lead to a porous permeable oxide layer with no protective properties. Brooks [11] found through experiments that chlorine is one of the important factors for the destruction of the oxidation protective layer on the wall of water-cooled tubes. Gibb [12] proposed that the chlorine content of coal not exceeding 0.3% is a method for selecting coal to avoid corrosion of chlorine. A. Hernas et al. [13] studied the high-temperature corrosion mechanism of 2.25% Cr~18% Cr series power station boiler heat-resistant alloy steel by simulating the oxidizing atmosphere of chlorine-sulfur. The results show that the corrosion resistance of heat-resistant alloy steel Sex determines the Cr content in the steel. Although there have been many researches on high-temperature corrosion mechanism and some progress has been made, there is no consensus on the corrosion mechanism. Based on this, this paper selects 12Cr1MoV pipe as the research object and experimentally studied in H_2S and SO_2. The corrosion rate under two corrosive atmospheres was analyzed.

2. Experimental devices

The whole system includes three parts: a gas distribution device, a reaction device and an exhaust gas treatment device. The gas distribution device is composed of a gas cylinder, a mass flow meter, a gas mixing device and a pipeline, and the gas is controlled by the mass flow meter and then mixed into the reaction device. The reaction device is an electric heating tube furnace with a temperature control error of ±1℃, a maximum heating rate of 25℃/min, and a maximum operating temperature of 1400℃. The furnace is a quartz tube with an inner diameter of 50 mm. The sample is placed in a constant temperature section of the furnace at a low temperature, filled with an inert gas, then heated to a reaction temperature and then thermostated, and the reaction gas is introduced into the reaction with the sample. After a predetermined time of reaction, the inert gas is charged and cooled, and the sample is taken out for detection. The exhaust gas treatment system is a gas filtration system containing NaOH, which absorbs harmful gases remaining after the reaction.

Table 1. The main chemical composition quality score of the material in this paper/%.

Material	C	Si	Mn	Cr	Mo	V
12Cr1MoV	0.08~0.15	0.17~0.37	0.4~0.7	0.9~1.2	0.25~0.35	0.15~0.3

For better measurement, cleaning and processing and to weaken the influence of "border effect", the test pieces are machined by wire cutting with a size of 10 mm × 10 mm × 2 mm and with an accuracy of 0.001 mm in the test. The cut test pieces were smoothed with 800-mesh sandpaper, degreased with an anhydrous ethanol solution, and then blotted dry with a filter paper. After wrapping the clean paper, it is placed in a drying oven at 70℃ and dried at a constant temperature for use. The exact dimensions of the specimen were measured using a vernier caliper.

3. Experimental results and discussion

3.1. Corrosion rate in the air atmosphere

In order to characterize the corrosion rate under different working conditions, the unit time is defined, and the corrosion weight per unit area is the corrosion rate. Figure 1 shows the results of corrosion experiments of 12Cr1MoV under air atmosphere, in which the vertical axis on the left is the weight per unit area and the horizontal axis is the corrosion time. Considering that the sub-critical boiler water wall temperature is in the range of 400-540℃, the temperature conditions of the experiment in this paper are also selected in this range, as close as possible to the actual working conditions on site. It can be seen that at the three temperatures of 400, 450, 500℃, as the corrosion time increases, the weight gain per unit area increases at the beginning, and the subsequent increase is gentle, showing a parabolic growth law. Moreover, the higher the temperature, the bigger the corrosion gain. At the 168h corrosion time, the corrosion weight gain per unit area at 400℃ is 1.2 $mg \cdot cm^{-2}$, and the corresponding

value at 500℃ is 4.8 mg·cm^{-2}, which is 4 times the corresponding value of 400℃. To further quantitatively describe the relationship between corrosion rate and corrosion time, the unit weight is squared to obtain a quantitative relationship model at three temperatures, as shown in the Figure 1.

The unit weight gain squared y^2 and the corrosion time h show a good linear relationship. The quantitative relationship model at three temperatures is shown in Table 2. The correlation coefficient R^2 is above 0.98. The slope of the fitted line can reflect the magnitude of the corrosion rate.

Table 2. The relationship between the square area weight gain y^2 and the corrosion time h at three temperatures.

Temperature	400℃	450℃	500℃
Air	$y^2 = 0.01152t - 0.02568$ $R^2 = 0.9882$	$y^2 = 0.0403t - 0.1889$ $R^2 = 0.9944$	$y^2 = 0.13211t - 0.52083$ $R^2 = 0.9977$

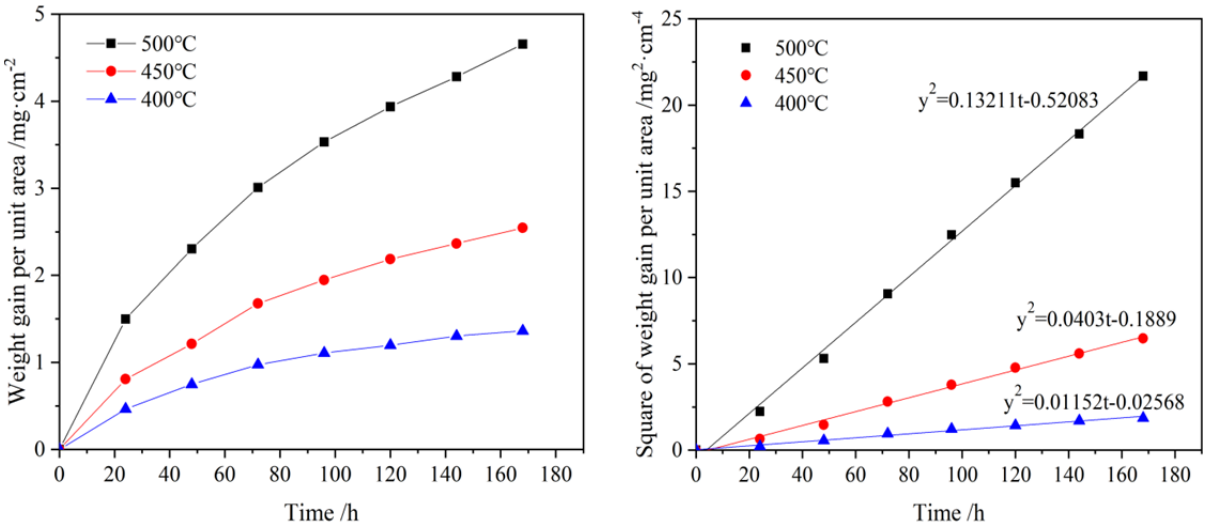

Figure 1. Corrosion experiment of 12Cr1MoV in the air atmosphere.

3.2. Corrosion rate in the H_2S atmosphere

Using the above data processing method, the relationship between the square of weight gain per unit area y^2 and the corrosion time h under different concentrations of H_2S atmosphere can be obtained, as shown in Figure 2. Since the slope of the fitted straight line representing the corrosion rate, it can be seen that the higher the temperature, the greater the corrosion rate. Under the same temperature condition, the corrosion rate increases significantly with the increase of H_2S concentration. Taking 400℃ as an example, the slope of the fitted line of 0.02% H_2S atmosphere is 0.04, while the slope of the fitted line of 0.1% H_2S atmosphere is 0.44, which is 11 times that of the former. Moreover, comparing all the four kinds of H_2S atmospheres with the air atmosphere, the corrosion rate in the H_2S atmosphere is significantly faster. Taking the 400℃ operating condition as an example, the slope of air atmosphere fitting linear is 0.01, and the slope of 0.02% H_2S atmosphere fitting linear is it's 4 times.

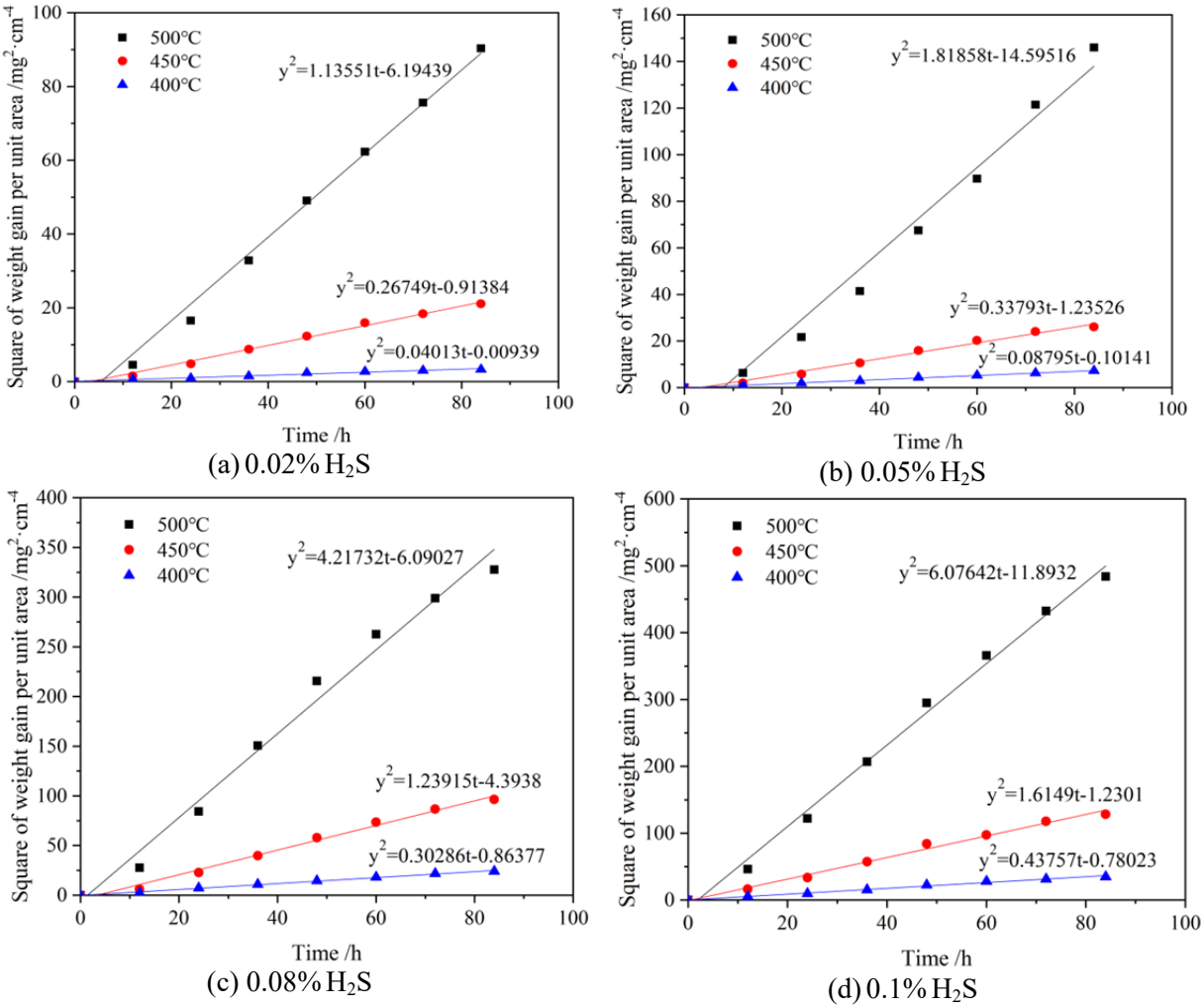

Figure 2. Corrosion experiment of 12Cr1MoV under H_2S atmosphere.

3.3. Corrosion rate in the SO_2 atmosphere

Similarly, using the above data processing method, the relationship between the square of weight gain per unit area y^2 and the corrosion time h under different concentrations of SO_2 atmosphere can be obtained, as shown in Figure 3: the higher the temperature, the greater the corrosion rate. At the same condition of temperature, the corrosion rate increases significantly with the increase of SO_2 concentration. Taking 500℃ as an example, the slope of 0.02% SO_2 atmosphere fitting linear is 0.03, while the slope of 0.1% SO_2 atmosphere fitting linear is 0.07, which is 2.3 times of the former. In addition, comparing all the four kinds of SO_2 atmospheres with the air atmosphere, the corrosion rate under the SO_2 atmosphere is smaller than the corrosion rate under the air atmosphere. Similarly, taken the 500℃ operating condition as an example, the slope of the air atmosphere fitting line is 0.13, which is 4.3 times as the slope of the fitted line of the 0.02% SO_2 atmosphere.

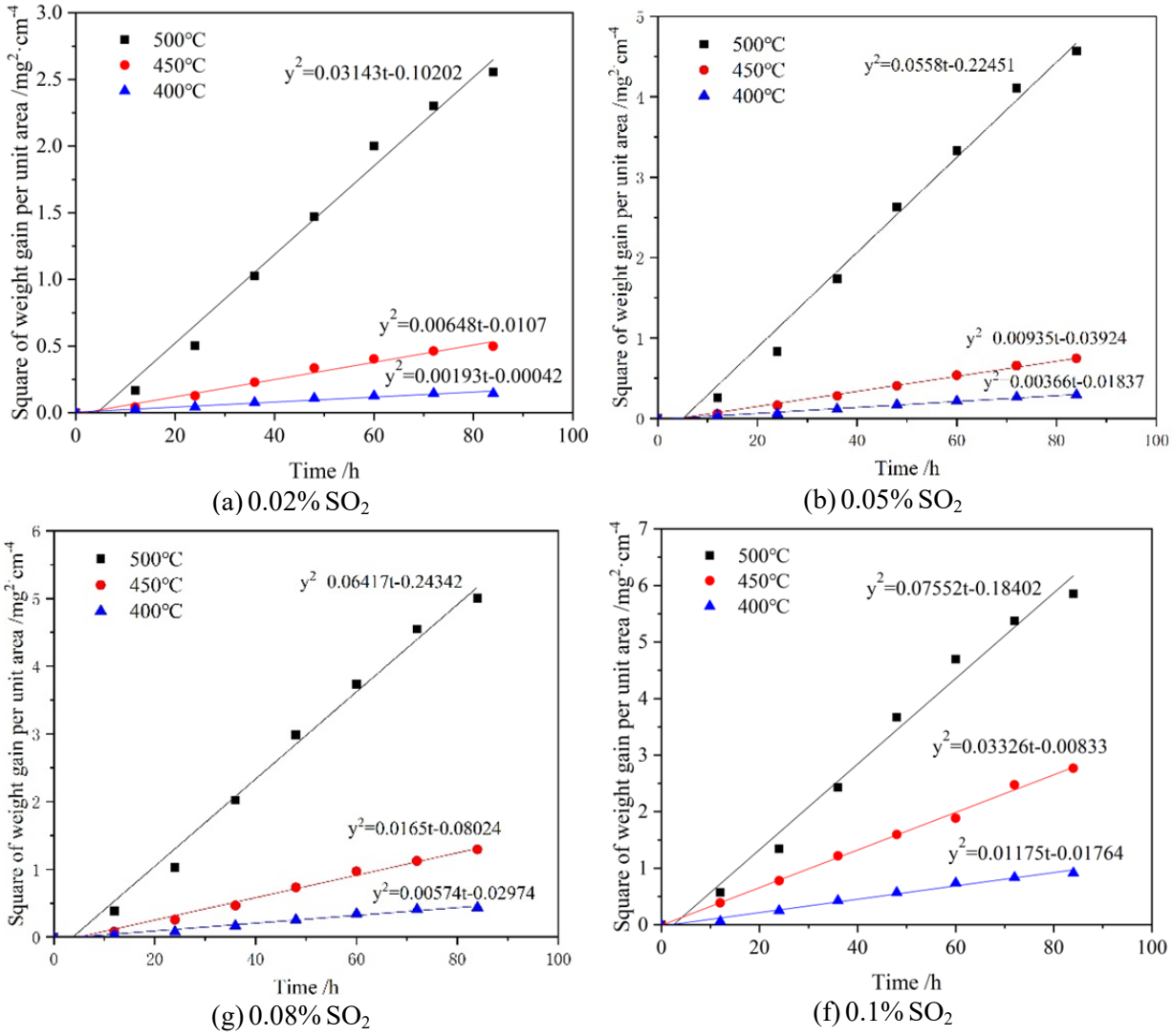

Figure 3. Corrosion experiment of 12Cr1MoV under the SO_2 atmosphere.

4. Corrosion product morphology and composition of 12Cr1MoV

In order to reveal the microscopic mechanism of corrosion, the etched test piece was observed by a scanning electron microscope with an energy spectrum analyzer, and the surface topography of 10,000 times by SEM was shown in Figure 4.

4.1. Effect of temperature on the morphology of corrosion products

Figure 4(a) (d), (b) (e), (c) (f) are the surface topographies of the products after corrosion at different temperatures (400 and 500℃) in three atmospheres (Air, 0.08% H_2S and 0.05% H_2S). By comparing the two morphologies in the group, it can be seen that at 400°C, a rough undulating oxide film covers the three groups of surfaces, and the needle-like or feather-like crystals are interwoven into a network. These non-protective oxide films cannot prevent further corrosion. However, the surface crystal at 500°C is coarser and flakier. Compared with 400°C, it becomes porous, indicating that the corrosion is more intense, and the corrosive medium can be further corroded through the pores, especially in the H_2S atmosphere. The surface crystals are staggered and ruptured, and the laminates are convex and have a clear tendency to fall off.

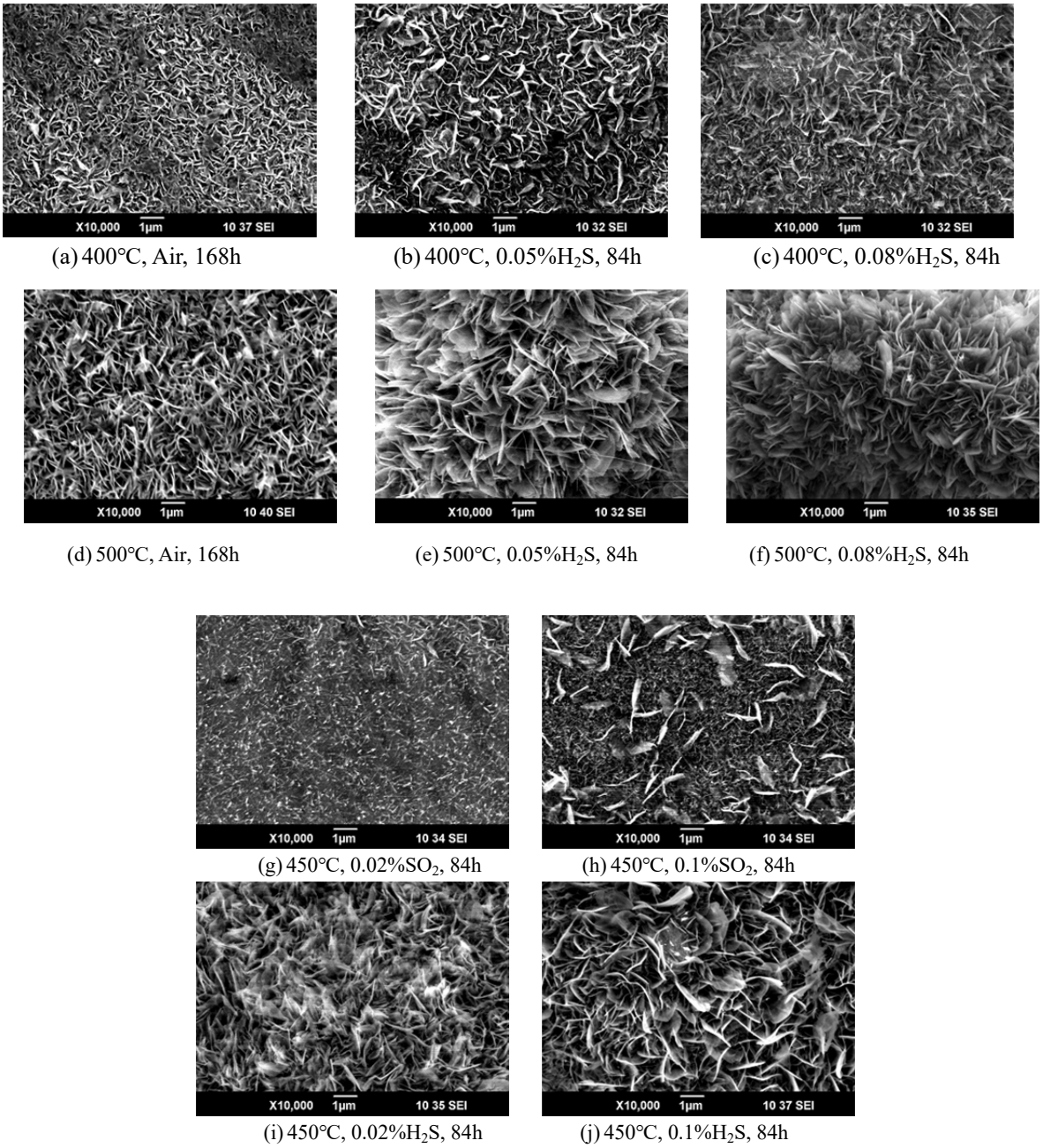

(a) 400℃, Air, 168h (b) 400℃, 0.05%H_2S, 84h (c) 400℃, 0.08%H_2S, 84h

(d) 500℃, Air, 168h (e) 500℃, 0.05%H_2S, 84h (f) 500℃, 0.08%H_2S, 84h

(g) 450℃, 0.02%SO_2, 84h (h) 450℃, 0.1%SO_2, 84h

(i) 450℃, 0.02%H_2S, 84h (j) 450℃, 0.1%H_2S, 84h

Figure 4. Surface morphology of the product under different temperature atmospheres.

4.2. Effect of atmosphere on the morphology of corrosion products

Figure 4(b) (c), (e) (f), (i) (j) are the surface topography of the products after corrosion at the same temperature and different concentrations of H_2S. It can be seen from the comparison that as the concentration of H_2S increases, the surface of the oxide film changes from needle-like to feather-like and lamellar. The volume of the crystal is getting larger while the cracks and the pores are getting denser, and the boundaries between crystals are getting blurred than before, indicating that the corrosion is intensified and the protection ability of the oxide film is decreased.

Figure 4(g), (h) are the surface topographies of the products after corrosion at different concentration of SO_2 at the same temperature. We can see from the comparison that a large number of fine needle crystals in the 0.02% SO_2 condition covers the surface, but the surface is flat and dense,

which can effectively prevent further corrosion. While in the 0.1% SO_2 condition, most of the surface is still made of dense needles, but some of the crystals grow significantly thicker and protrude from the surface, which destroys the overall compactness of the oxide film and thus reduces the corrosion resistance.

Figure 4(a), (b) and (h) are the surface topographies of conditions that 168h at 400°C under air, 84h at 400°C under 0.05% H_2S and 84h at 450℃ under 0.1% SO_2. Since the corrosive medium content, temperature and corrosion time are not uniform, it can not be compared in a strict sense, but the general trend can be seen: a dense oxide film composed of fine needles under air, and a coarse overlapping feather or lamellar crystals under H_2S atmosphere, and very fine needle-like crystals under SO_2 atmosphere. Even if a small portion of the dense oxide film is destroyed at a higher SO_2 concentration, so it can be inferred that the oxide film protection in the test atmosphere is SO_2 atmosphere>air>H_2S atmosphere. While the oxygen content in the air is much higher than the SO_2 and H_2S contents in the test atmosphere, the corrosion capacity at the same concentration is H_2S>SO_2>O_2.

4.3. Surface composition of corrosion products

In order to qualitatively analyze the test results, an energy spectrum analysis test was carried out using an equipped X-ray energy spectrometer (EDS) while performing a scanning electron microscope SEM test. The surface element distribution of the sample after corrosion is shown in Table 3. Because the corrosive medium mainly contains S and O, and the metal substrate mainly contains Fe, Cr, Mo, and V, therefore focus is to observe the content of these elements.

Table 3. Surface element distribution of products under different temperature atmospheres.

Elements	O		Fe		Cr		Mo		V		S	
Units	at.%	wt.%	at.%	wt.%	at.%	wt.%	at.%	wt.%	at.%	wt.%	at.%	wt.%
400℃Air	60.9	30.48	37.95	66.31	0	0.24	1	2.94	0	0.03	0	0
500℃Air	62.03	31.81	37.68	67.45	0.13	0.17	0.18	0.56	0	0	0	0
400℃ 0.08%H_2S	61.74	31.65	38	68.01	0.1	0.16	0	0	0.01	0.02	0.15	0.15
500℃ 0.08%H_2S	61.95	31.82	37.47	67.18	0.38	0.64	0.05	0.15	0.11	0.18	0.03	0.03
400℃ 0.05%H_2S	61.27	31.21	38.51	68.48	0.12	0.2	0.01	0.31	0	0	0.09	0.1
500℃ 0.05%H_2S	61.61	31.44	38.01	67.7	0.08	0.13	0.05	0.15	0.01	0.02	0.08	0.08
450℃ 0.02%SO_2	61.63	31.23	37.22	65.84	0.19	0.31	0.82	2.48	0	0	0.14	0.14
450℃ 0.1%SO_2	61.38	31.31	38.34	68.26	0.2	0.32	0	0	0.03	0.05	0.06	0.06
450℃ 0.02%H_2S	61.74	31.65	38	68.01	0.1	0.16	0	0	0.01	0.02	0.15	0.15
450℃ 0.1%H_2S	60.69	30.66	39.01	68.81	0.11	0.19	0.07	0.21	0.03	0.04	0.09	0.09

It can be seen from Table 3 that the surface of the product is mainly iron and oxygen, chromium, molybdenum and vanadium are all trace amounts, while the surface of the sulfur-containing atmosphere also contains trace amounts of S. From the table, it can be calculated that the proportion of Fe in the surface metal element is about 0.954~1 (see Table 4), while the mass content of iron in the 12Cr1MoV substrate is above 97%, so it is understandable that the surface metal element is mainly Fe.

The atomic ratio of M/O in metal M_3O_4 is 1.33, and the atomic ratio of M/O in metal M_2O_3 is 1.5. Calculating the atomic ratio of surface metal elements and non-metal elements (see Table 3), it is found that the (Fe+Cr+Mo+V)/(O+S) atomic ratio is about 1.55~1.63, and the Fe/O atomic ratio is about 1.59 ~1.66, even higher than M_2O_3. The difference may be the formation of higher-priced oxides such as MoO_2, MoO_3, V_2O_5, etc., may also be caused by measurement errors. Assuming that all elemental oxides take a high valence state, theoretically, the maximum number of O atoms is required to be 1.5Fe+1.5Cr+3Mo+2.5V. After calculating the atomic ratio O/(1.5Fe+1.5Cr+3Mo+2.5V), it is found to be greater than 1, which is not in accordance with common sense and can be determined as a measurement error. It can also be confirmed that the main component of the surface is Fe_2O_3, and a small amount of other metal oxides and the sulfur-containing atmosphere also contains trace amounts of sulfides.

It can be seen from Table 4 that there are some differences in the surface element content under different atmospheres and different temperatures, but the change is not large. Considering the existence of measurement error, it is difficult to distinguish the surface element content with the change of atmosphere and temperature. It can be considered to be substantially unchanged, and 95% or more of the surface component is Fe_2O_3.

Table 4. The proportion of surface element content of products under different temperature atmospheres.

Element ratio	$\frac{Fe}{Fe+Cr+Mo+V}$	$\frac{Fe+Cr+Mo+V}{O+S}$	$\frac{O}{1.5Fe+1.5Cr+3Mo+2.5V}$	$\frac{Fe}{O}$
Units	wt./wt.	at. /at.	at. /at.	at. /at.
400℃ Air	0.9538	1.56	1.01	1.60
500℃ Air	0.9893	1.63	1.08	1.65
400℃ 0.08% H_2S	0.9974	1.62	1.08	1.62
500℃ 0.08% H_2S	0.9858	1.63	1.08	1.65
400℃ 0.05% H_2S	0.9926	1.59	1.06	1.59
500℃ 0.05% H_2S	0.9956	1.62	1.08	1.62
450℃ 0.02% SO_2	0.9593	1.62	1.05	1.66
450℃ 0.1% SO_2	0.9946	1.59	1.06	1.60
450℃ 0.02% H_2S	0.9974	1.62	1.08	1.62
450℃ 0.1% H_2S	0.9936	1.55	1.03	1.56

5. Conclusions

The corrosion behavior of 12Cr1MoV steel under H_2S, SO_2 and air atmosphere at 400, 450, 500℃ is systematically studied, and analyzed the high-temperature corrosion mechanism of gases in combination with corrosion topography. The main conclusions are as follows:

(1) It is found that the corrosion rate is highest in the H_2S atmosphere, and slowest in the SO_2 atmosphere. The corrosion rate is moderate in the air atmosphere. By analyzing the influence of temperature on the corrosion rate, it is found that the corrosion rate is roughly doubled for every 50℃ interval at 400-500℃.

(2) The surface morphologies of 12Cr1MoV after corrosion were analyzed. It is a dense needle-shaped dense oxide film under air, a coarse porous oxide film composed of coarsely overlapping feathers or lamellar crystals under the H_2S atmosphere. Otherwise, under the SO2 atmosphere, there exists a very dense and smooth oxide film composed of very fine needle-like crystals over the samples.

At higher SO_2 concentrations, some coarse feathery crystals appear on the surface. From the compactness, roughness and porosity of the oxide film, it can be inferred that the oxide film protection in the test atmosphere is SO_2 atmosphere>air>H_2S atmosphere. And since the oxygen content in the air is much higher than the SO_2 and H_2S content in the test atmosphere, Therefore, the corrosion capacity at the same concentration is H_2S>SO_2>O_2.

(3) Comparing the surface topographies of 12Cr1MoV that after corrosion in the same atmosphere, it is found that the surface of 12Cr1MoV corrosion products is mainly Fe_2O_3. In addition, the higher the temperature and the concentration of the corrosive medium, the larger the crystal after corrosion, the coarser the surface, the greater the tendency of the oxide film to crack and peel, and the lower the corrosion resistance.

From the above, in the actual operation of the power plant boiler, the wall temperature and the concentration of H_2S near the wall should be strictly monitored to reduce the probability of high-temperature corrosion.

References

[1] Cain C,Nelson W 1961 Corrosion of Superheaters and Reheaters of Pulverized CoalFired Boilers-II.*Trans.ASME.J.Engng for Power* **10** 468-474
[2] Nelson W,Cain C 1960 Corrosion of Superheaters and Reheaters of Pulverized CoalFired Boilers.*Trans.ASME* **82** 194-204
[3] Hedly AB 1967 Factors Affecting the Formation of Sulfur Trioxide in Flue Gases *Inst.Fuel* **40** 142
[4] Krause HH,Levy A and Reid WT 1968 Sulfur oxide reactions:Sulfur andmicroprobe studies of corrosion and deposits *Trans.ASME,J.Engng Power* **90** Series A:38-44
[5] Schofield,Keith 2003 A new method to minimize high-temperature corrosion resultingfrom alkali sulfate and chloride deposition in combustion systems *Energy and Fuels* **17(1)** 191-203.
[6] Latham E,Meadowcroft DB and Pinder L 1989 The effects of coal chlorine on fireside corrosion,Proceedings of the Incinerating Municalpal and Industrial Waste-Fireside Problems and Prospect for Improvement Conference.Sheraton Palm Coast,Florida,Hemisphere Press 47-117
[7] Krause HH,Vaughan DA,Miller PD 1974 Corrosion and deposits from combustion of solid waste,part II-chloride effects on boiler tube and scrubber metals *Engng for Power* **96(3)** 216-222
[8] Krause HH,Vaughan DA,Boyd KW 1975 Corrosion and deposits from combustion of solid waste,part III-effects of sulfur on boiler tube metals *Engng for Power* **97(3)** 448-452
[9] Krause HH 1989 Corrosion by chlorine in waste-fueled boilers,Proceedings of the Incinerating Municipal and Industrial Waste-Fireside Problems and Prospect for Improvement Conference. W.Bryers(ed.),Sheraton Palm Coast,Florida, Hemisphere Press 145-159
[10] Lee DJ and Whitehead ME. 1983 The influence of gas and deposit chemistry of the fireside corrosion of furnace wall tubes in coal-fired boilers,Proceedings of the Engineering Foundation Conference on Fouling of Heat Exchangers.W.Bryers (ed.).White Haven,PA,1981;Engineering Foundation,New York City Publication No.83-01, 69-104.
[11] Brooks S and Meadowcroft DB 1983 Corrosion Resistant Materials for Coal Conversion systems *Applied Science Publishers,London* 105
[12] Gibb WH,Angus JR 1983 The release of potassium from coal during bomb combustion *Journal of the Institute of Energy* **56(9)** 149-157
[13] A.Hernas, M.Imosa, B.Formanek, J.Cizner 2004 High-temperature chlorine–sulfur corrosion of heat-resisting steels *Journal of Materials Processing Technology* **57(8)** 348-353